Development, validation, and sensitivity analysis of circumglobal CO_2 air-sea gas transfer velocity and its parameterisations with a spectral wave model

Andrew W. Smith[1], Adrian H. Callaghan[1] and Jean-Raymond Bidlot[2]
[1]Imperial College London [2]European Centre for Medium-Range Weather Forecasts

Postdoctoral Fellow Interview, April 19, 2024 | University of Rhode Island, Narragansett, RI

THE UNIVERSITY OF RHODE ISLAND

ECMWF European Centre for Medium-Range Weather Forecasts

UKRI Natural Environment Research Council

Air-Sea Fluxes

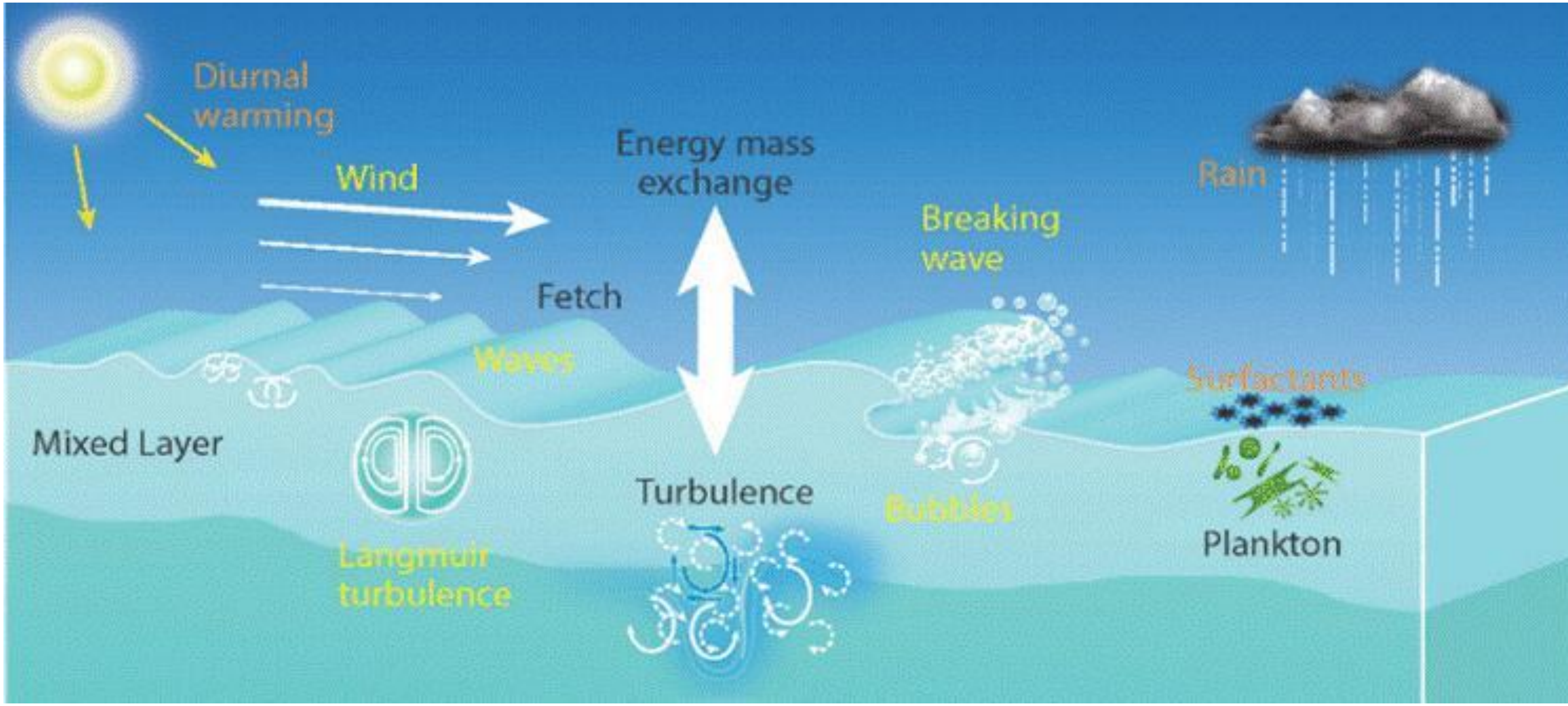

Momentum, heat, material and gas exchanged between atmosphere, waves, and ocean through dynamic and thermodynamic processes

Diffusion • Wave growth and breaking ⟶ gas flux

Bubbles, sea spray, spume facilitate exchange and impact up-scale budgets

Air-sea gas fluxes ⟶ global climate

Notable Gases and their Importance

N_2 (62.6 %)

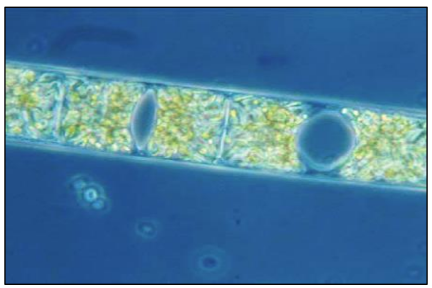

1. Fixation by marine bacteria

NH_4^+

NO_2^{2-}

NO_3^- →

O_2 (34.3 %)

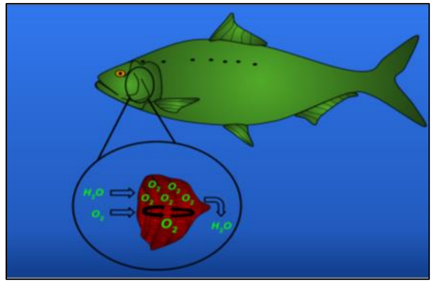

1. Aerobic respiration
2. Photosynthesis (byproduct)

CO_2 (1.4 %)

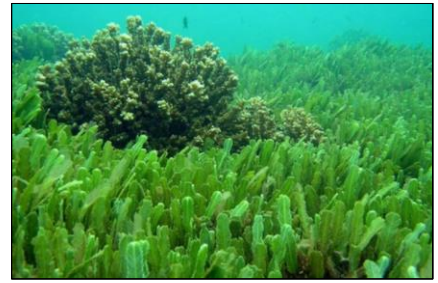

1. Aerobic respiration
2. Photosynthesis (reactant)
3. Carbon cycle/ loading

CH_4 (0.0004 %)

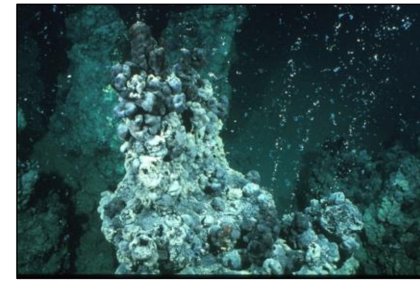

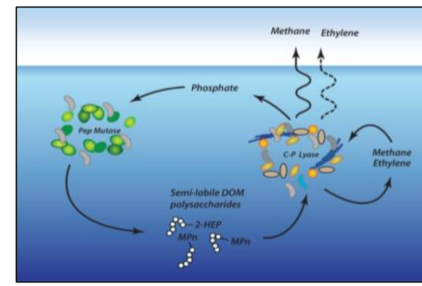

1. Benthic bacterial decomposition
2. Hydrothermal release
3. Methanogenesis

$CO_2 + H_20$	↔	H_2CO_3	↔	$H^+ + HCO_3^-$	↔	$2H^+ + CO_3^{2-}$
(dissolved) 1 %		(carbonic acid)		(bicarbonate) 92 %		(carbonate) 7 %

Scientific Objectives

1. Develop a hybrid gas transfer velocity parameterization with bubble-mediated gas exchange linked explicitly to breaking wave energy dissipation

   Diffusive gas flux
   Bubble-mediated gas flux

2. Evaluate our and other extant parameterisations using outputs from a wind-forced spectral wave model, and compare with field measurements

   9 global cruises (2007-2019)

3. Identify sources of parameterisation success, uncertainty and error considering physical and chemical processes

   Wind-wave momentum flux
   Wave-ocean energy dissipation (wave breaking)
   Bubbles and surfactants

Field Data: Global Cruises

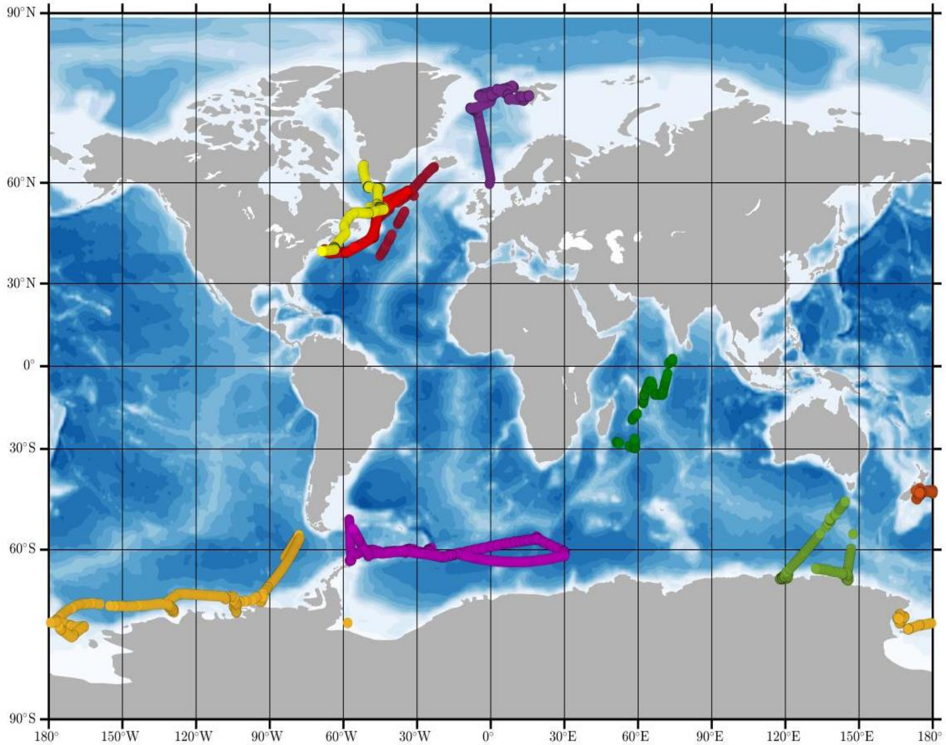

		Measurements (#)
1	R/V Knorr (2007)	61
2	R/V Knorr (2011)	215
3	SOAP (2012)	220
4	NBP-1210 (2013)	234
5	HiWinGS (2013)	529
6	NBP-1402 (2014)	68
7	SO-234/235 (2014)	74
8	ANDREXII (2019)	199
9	JR18007 (2019)	293

Measurements / Methods

1. **4 June 2007 – 29 August 2019**: 9 cruises, hourly data in various ocean basins, water depths, time of year, fetch, and wind-wave conditions

2. High-quality **eddy covariance CO_2 fluxes** and **air-sea CO_2 concentration gradients** via closed-path infrared gas analyzers (LI-COR Li-7200, Li-7500) or cavity-ring down mass spectrometers (Picarro G1301-f, G2311-f)

Field Data: Global Cruises

Bivariate PDFs & Data Density

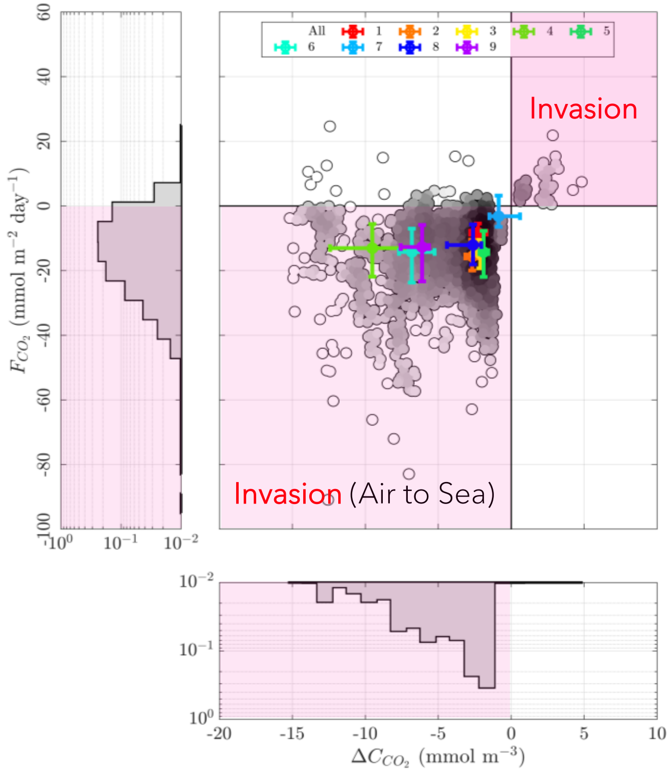

Gas Transfer Velocity *k* (at *Sc* = 660)

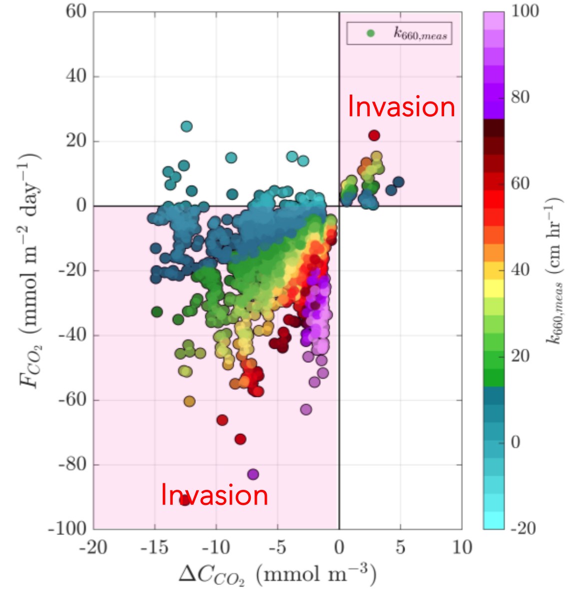

Measurements / Methods

3

Gas transfer velocity of CO_2 via CO_2 fluxes and concentration gradients; met-ocean state variables also measured in each cruise (u_*, U_{10N}, SST, solubility, Schmidt number)

$$k = \frac{F_{CO_2}}{\Delta C_{CO_2}} = \frac{F_{CO_2}}{S(\Delta f_{CO_2})}$$

Spectral Wave Model: ECMWF ERA-5H ecWAM

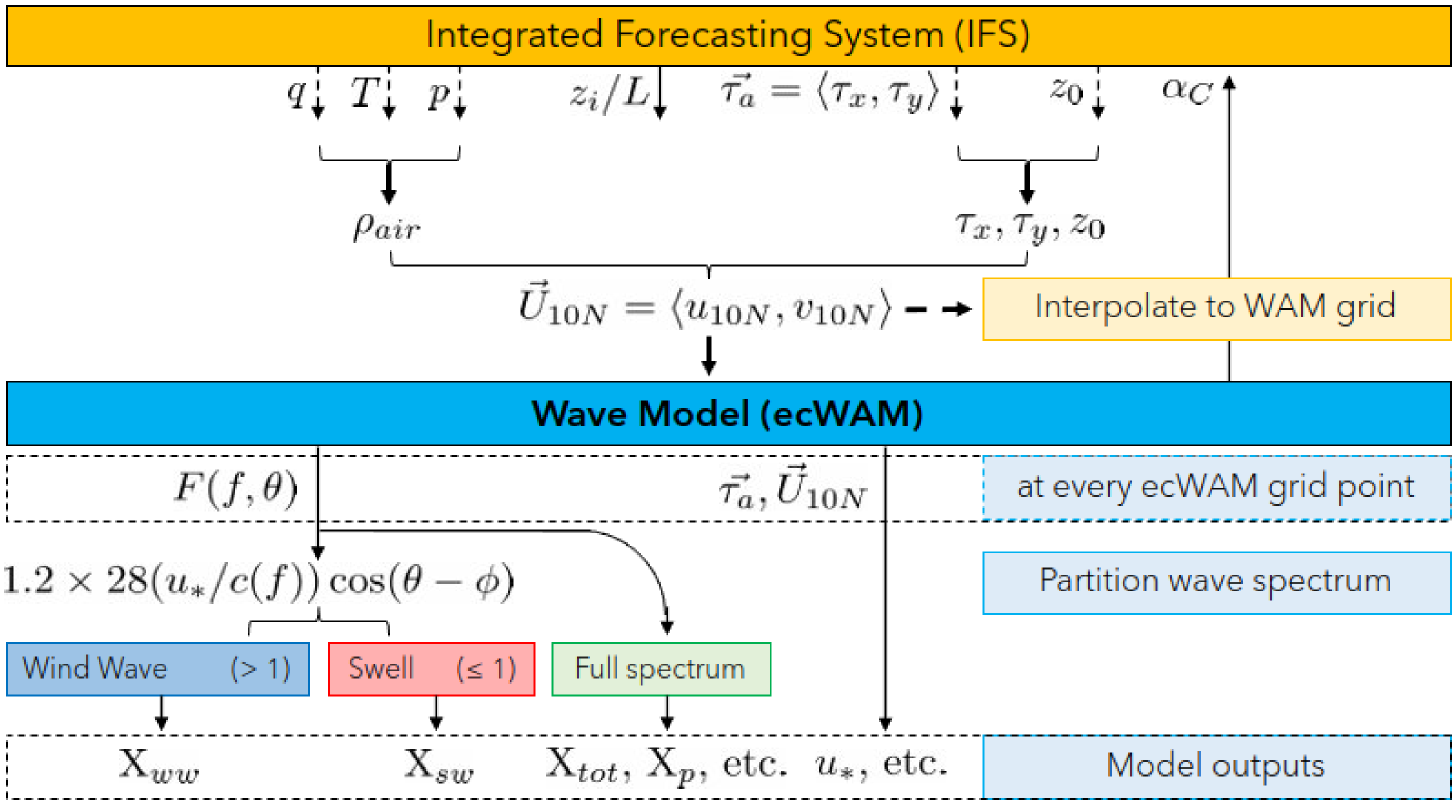

Model Details

1. Global wave model forced by hourly **ERA-5** wind (U_{10N}), surface air density, gustiness, and sea ice cover

2. **14** km × **14** km (**0.125°** x **0.125°**) spatial resolution
36 frequencies (f_{min} = 0.035 Hz) x **36** directions

Spectral Wave Model: ECMWF ERA-5H ecWAM

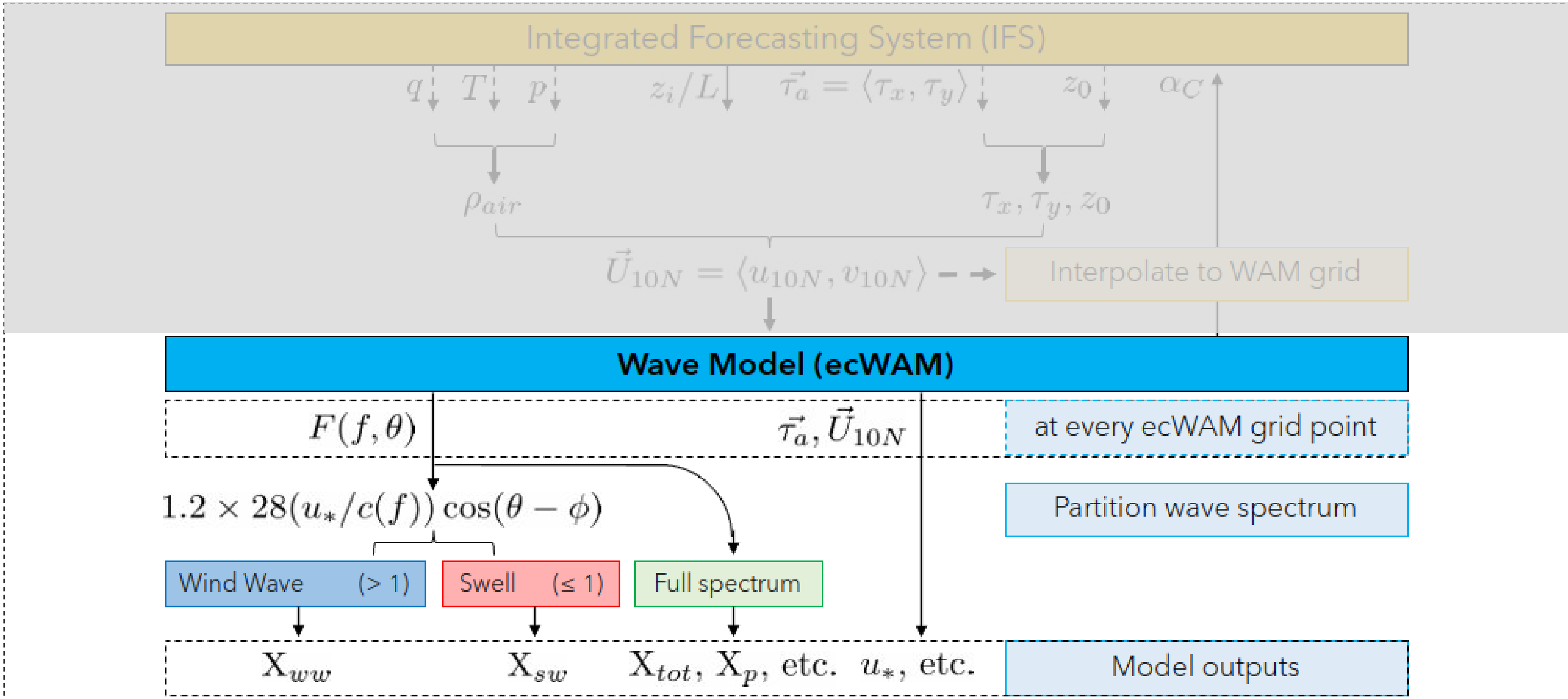

Model Details

3 **4 June 2007 – 29 August 2019**: 1-hour outputs
Interpolated in space and time to all cruise coordinates

4 **2-D wave spectrum** ***F*****(*****f*****, θ)** and **total atmospheric stress** $\boldsymbol{\tau}_a$ calculated at each model grid-point

Results: Parameterising Gas Transfer Velocity

Operational (Full) and Hybrid Forms

$$\boxed{k = \frac{F_{CO_2}}{S(\Delta f_{CO_2})}} \boxed{= k_s + k_b}$$

Diffusive Gas Transfer Velocity

$$k_s = \frac{D}{\delta z} \propto \left[(\varepsilon\nu)^m \cdot \left(\frac{\nu}{D}\right)^n\right] \simeq \left[(\varepsilon\nu)^m \cdot Sc^n\right]$$

Bubble-Mediated Gas Transfer Velocity

$$k_b = \frac{\int_0^\infty V(r)Q(r)E(r)dr}{\alpha} = \frac{V_b}{\alpha}$$

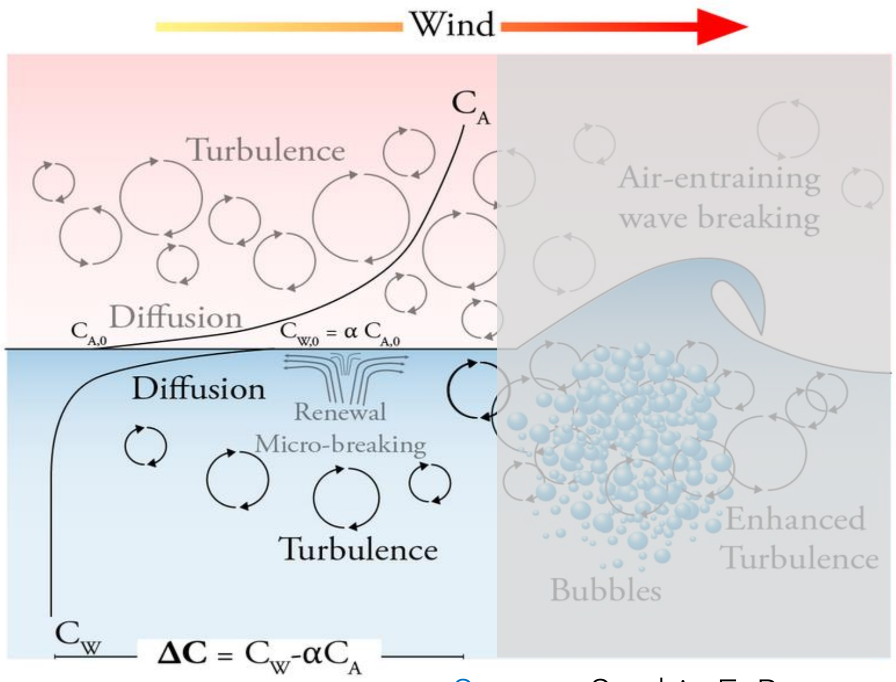

Source: Sophia E. Brumer

Results: Parameterising Gas Transfer Velocity

Operational (Full) and Hybrid Forms

$$\boxed{k = \frac{F_{CO_2}}{S(\Delta f_{CO_2})}} = k_s + k_b$$

Diffusive Gas Transfer Velocity

$$k_s = \frac{D}{\delta z} \propto \left[(\varepsilon\nu)^m \cdot \left(\frac{\nu}{D}\right)^n\right] \simeq \left[(\varepsilon\nu)^m \cdot Sc^n\right]$$

Bubble-Mediated Gas Transfer Velocity

$$k_b = \frac{\int_0^\infty V(r)Q(r)E(r)dr}{\alpha} = \frac{V_b}{\alpha}$$

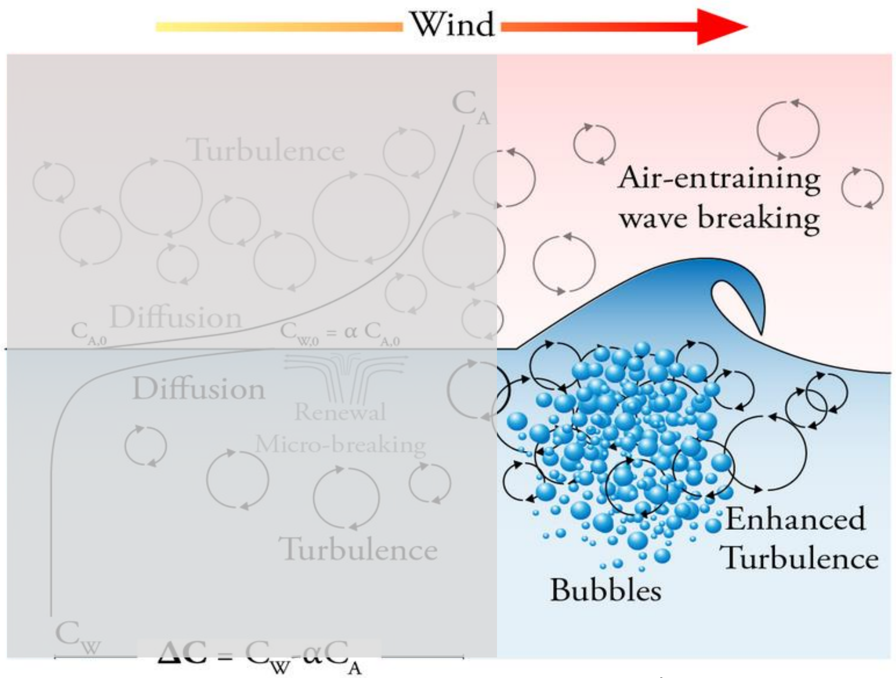

Source: Sophia E. Brumer

Results: Diffusive Gas Transfer Velocity

$$k_{s,param} = c_1 \boxed{u_{*\nu}}$$

$c_1 = 2.034 \times 10^{-4}$, optimised constant $[-]$ • $u_{*\nu}$, viscous friction velocity $[m\ s^{-1}]$

Atmospheric Stress Decomposition

$$\tau = \tau_\nu + \tau_f$$

Form Drag

$$\tau_f = \tau - \tau_\nu = \rho_a (u_*^2 - u_{*\nu}^2)$$

Viscous Friction Velocity via Mueller & Veron (2009)

$$u_{*\nu} = c_{d\nu}^{1/2} U_{10N} = \frac{\kappa}{\log(10/z_{o\nu})} U_{10N}$$

$$z_{o\nu} = \frac{0.11\nu_a}{u_{*\nu}}$$

Results: Diffusive Gas Transfer Velocity

$$k_{s,param} = \boxed{c_1 u_{*\nu}}$$

$c_1 = 2.034 \times 10^{-4}$, optimised constant $[-]$ • $u_{*\nu}$, viscous friction velocity $[m\ s^{-1}]$

Overview

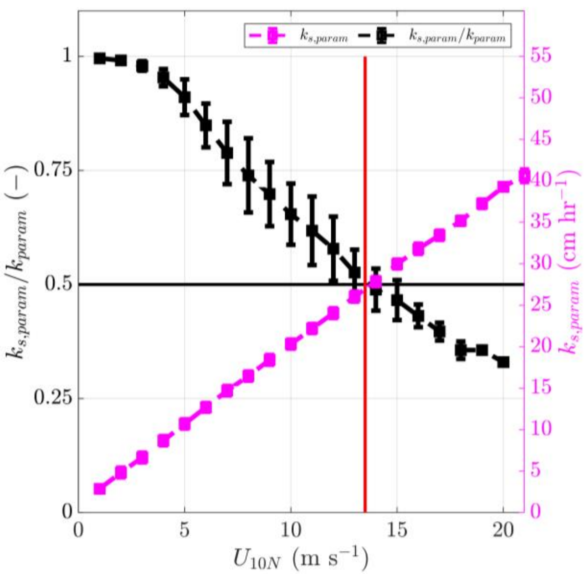

Log-Log vs. Measurements

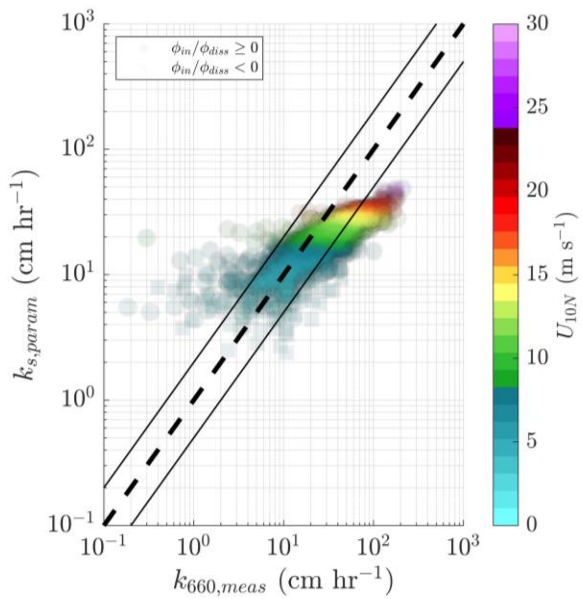

PDFs by Wave Age

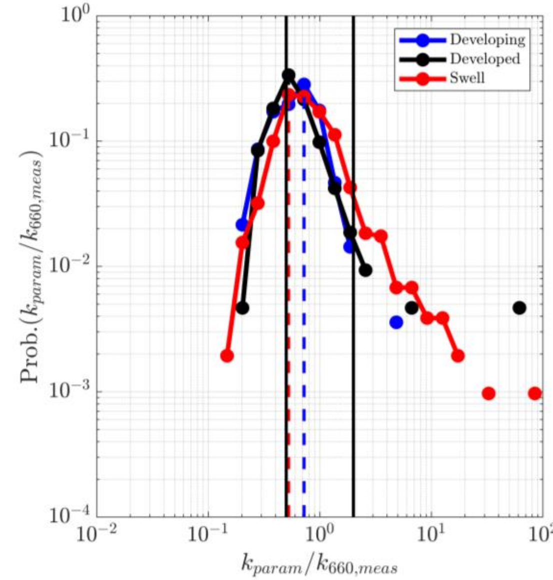

- Diffusive flux dominates gas transfer at wind speeds U_{10N} < 13.5 ms^{-1}
- $k_{s,param}$ approximately linear with U_{10N} via use of $u_{*\nu}$ (Fairall, et al. 2011)
- Diffusive flux alone insufficient at wind speeds U_{10N} > 8 ms^{-1}
- Across all wave-ages, PDFs show under-estimation of k_{660} by about 41 percent.

Results: Bubble-Mediated Gas Transfer Velocity

$$k_{b,param} = c_2 \frac{1}{\alpha} \boxed{a_{eff} \overline{w}_{ent} W_{growth}} \xi$$

$c_2 = 5.902$,optimised constant $[-]$ • a_{eff},effective void fraction $[-]$ • $\overline{w}_{ent}$,average entrainment velocity $[m\ s^{-1}]$
W_{growth}, growth-phase whitecap fraction $[-]$ • ξ, volume-weighted efficiency factor$[-]$

Growth-Phase Whitecap Fraction

$$W_{growth} = \frac{S_{wcap}}{\rho_w \Omega \hat{z}_p^*} = \frac{\tau_f c_{eff} \times (c_p U_{10N}^{-1})}{\rho_w \Omega \hat{z}_p^*}$$

Entrainment Velocity

$$\overline{w}_{ent} = \frac{\hat{z}_p^*}{T_{ww}}$$

Effective Air (Void) Fraction

$$a_{eff} = \frac{\int_0^{t_{A_0}} \alpha(t) V(t)\ dt}{\int_0^{t_{A_0}} V(t)\ dt}$$

Whitecap Foam Area Evolution

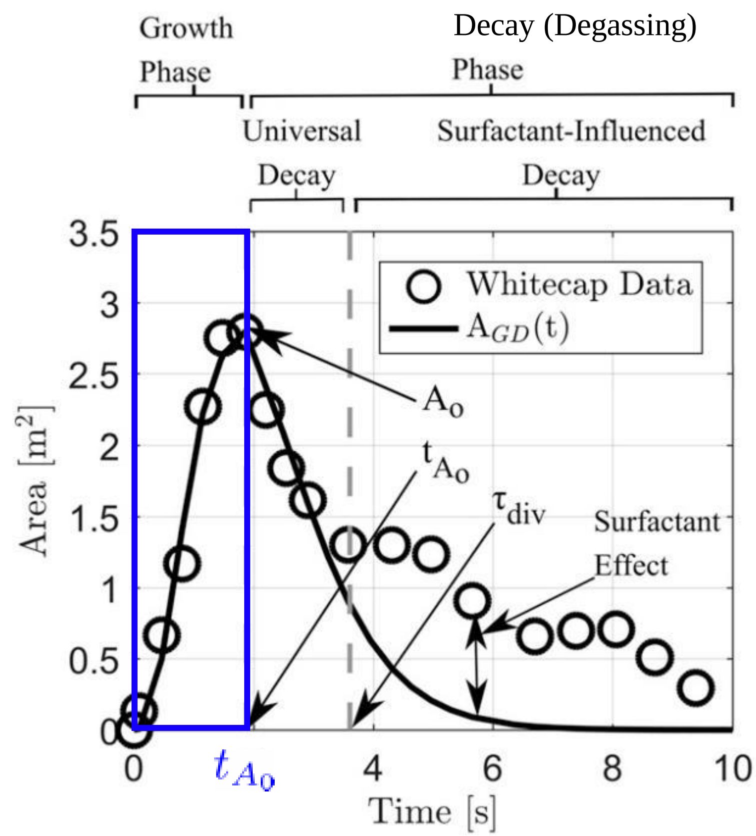

Results: Bubble-Mediated Gas Transfer Velocity

$$k_{b,param} = \boxed{c_2 \frac{1}{\alpha} a_{eff} \overline{w}_{ent} W_{growth}} \xi$$

$c_2 = 5.902$, optimised constant $[-]$ • a_{eff}, effective void fraction $[-]$ • $\overline{w}_{ent}$, average entrainment velocity $[m\ s^{-1}]$
W_{growth}, growth-phase whitecap fraction $[-]$ • ξ, volume-weighted efficiency factor $[-]$

Observed w_{ent} PDFs

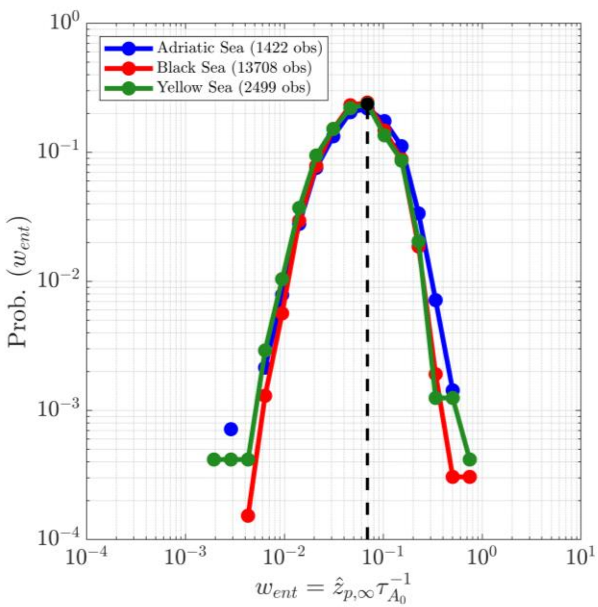

Modeled W_{growth}

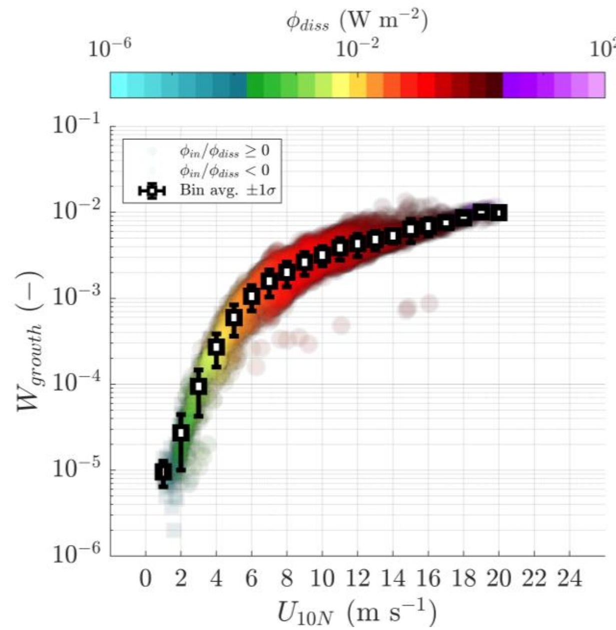

- $a_{eff} = 0.2$ choice within reported values from literature (0.012 - 0.37)
- $w_{ent} = 0.069$ from PDFs, 0.065 from MVCO, we use 0.066 m s^{-1}
- W_{growth} follows shape of observed $W(U_{10N})$ seen in literature
- Larger wave-ocean energy flux at higher winds and slope transition near $U_{10N} = 7$ m s^{-1}

Results: Bubble-Mediated Gas Transfer Velocity

$$k_{b,param} = \boxed{c_2 \frac{1}{\alpha} a_{eff} \overline{w}_{ent} W_{growth} \xi} \rightarrow \xi = \frac{\int_0^\infty V(r) E(r) dr}{\int_0^\infty V(r) dr}$$

$c_2 = 5.902$, optimised constant $[-]$ • a_{eff}, effective void fraction $[-]$ • $\overline{w}_{ent}$, average entrainment velocity $[m\ s^{-1}]$
W_{growth}, growth-phase whitecap fraction $[-]$ • ξ, volume-weighted efficiency factor $[-]$

Bubble size and volume distributions | Bubble efficiency | Volume-weighted Bubble efficiency

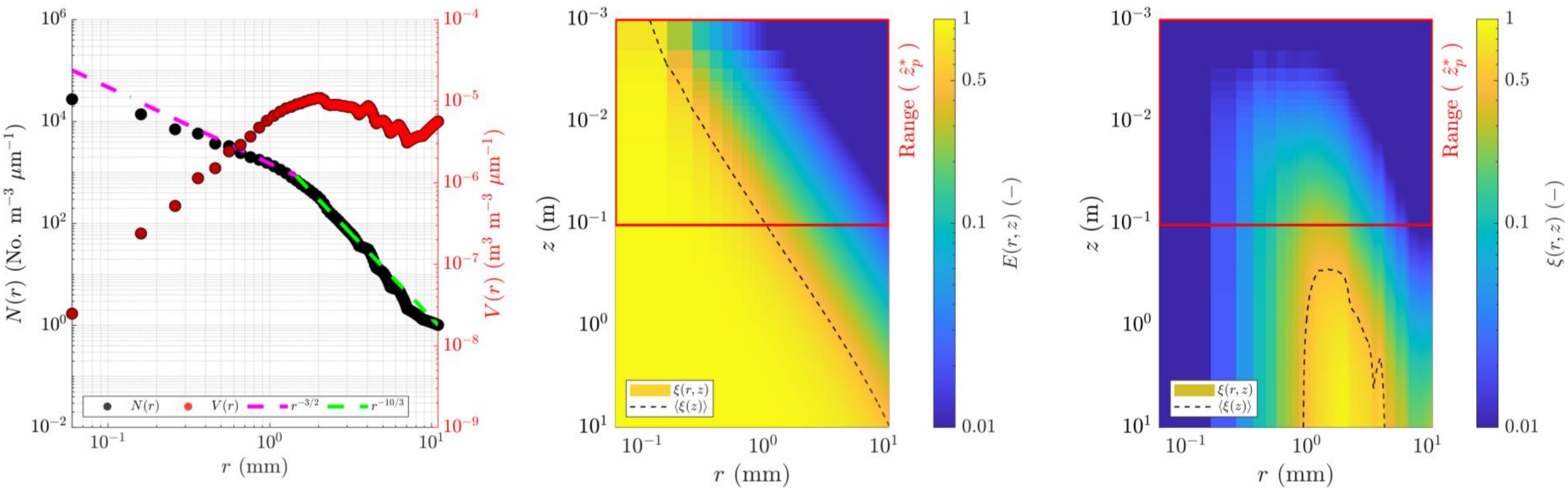

- N(r), V(r) from Deane & Stokes (2002): large bubbles near Hinze scale contribute most
- Bubble efficiency most sensitive to *r* at small *z*; bubbles at depth fully dissolve, efficient!
- Large bubbles fewer in number, but contribute more gas volume
- Most efficient bubbles *r* = 1-4.5 mm, at *z* ≥ 0.25 m; but occupy just 27.1% of *r*-*z* space

Results: Total Gas Transfer Velocity

$$k_{param} = \boxed{c_1} u_{*\nu} + \boxed{c_2} \frac{1}{\alpha} a_{eff} \overline{w}_{ent} \left(\frac{\tau_f c_{eff} \times (c_p U_{10N}^{-1})}{\rho_w \Omega \hat{z}_p^*} \right) \xi$$

*optimized via $\epsilon = \overline{|k_{660,meas} - (c_1 k_{s,param} + c_2 k_{b,param})|}$ such that $c_1, c_2 = \mathrm{fminsearch}(\epsilon)$

k_{660} (U_{10N})

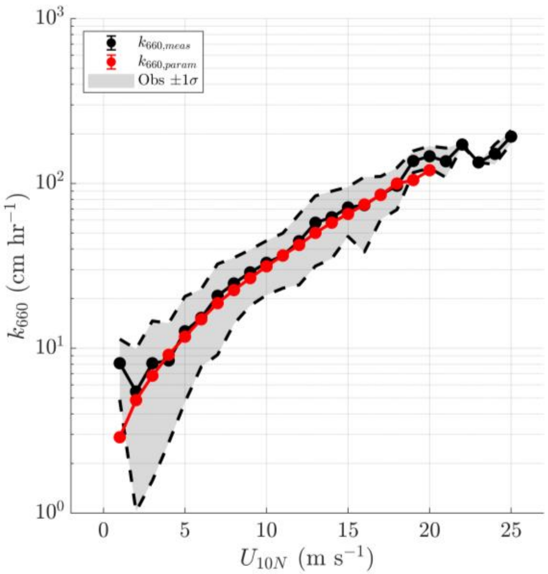

Parameterised vs. Observed k_{660}

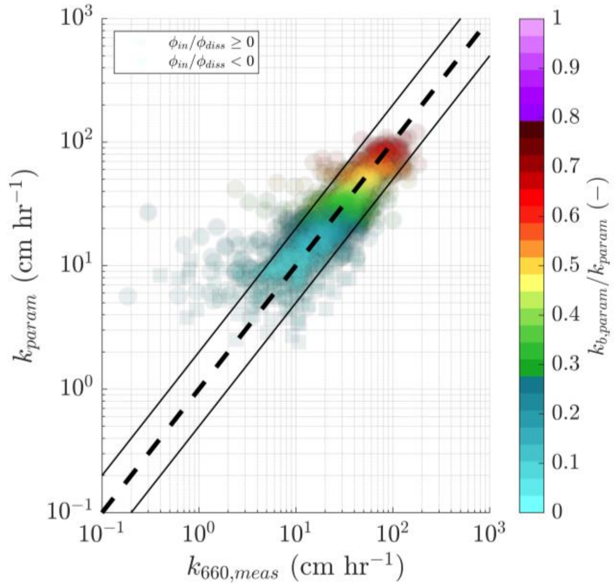

PDFs by Wave Age

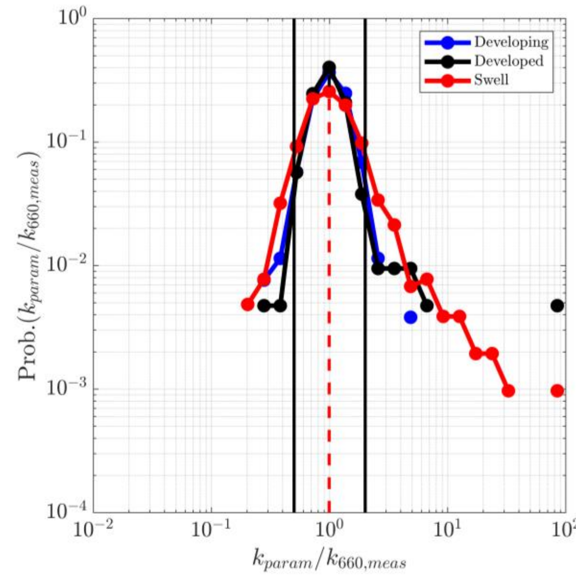

- Agreement between $k_{660,\,meas}$ and k_{param} good, median error 8.25%, $R^2 = 0.818$
- Largest errors: $U_{10N} < 3$ m s^{-1} and $U_{10N} \geq 19$ m s^{-1}
- Outliers comprise 13.49% of the data (outside 0.5×-2× solid black lines)
- PDFs narrower for wind sea (•, •) vs swell (•), although peak for all wave ages is 1

Results: Comparing Total Gas Transfer Velocity from Literature

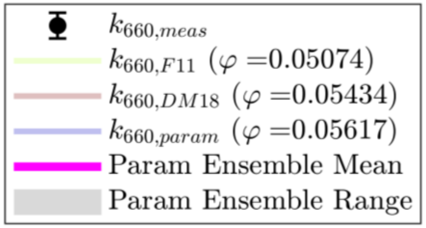

1. $k_{SC23} = c_1 u_{*\nu} + c_2 \frac{1}{\alpha} a_{eff} \overline{w}_{ent} \left(\frac{\tau_f c_{eff} \times (c_p U_{10N}^{-1})}{\rho_w \Omega \hat{z}_p^*} \right) \xi$ — Smith, et al. (2023; in prep.)
2. $k_{F11} = 37.5 A \psi u_{*\nu} + \frac{B V_o(T)}{\alpha(20)} f_{wh}(u_{*f})$ — Fairall, et al. (2011)
3. $k_{DM18} = A_{NB} u_* + A_B \frac{1}{\alpha} \left[u_*^{5/3} \sqrt{g H_s}^{4/3} \right]$ — Deike and Melville (2018)

k_{660} (U_{10N})

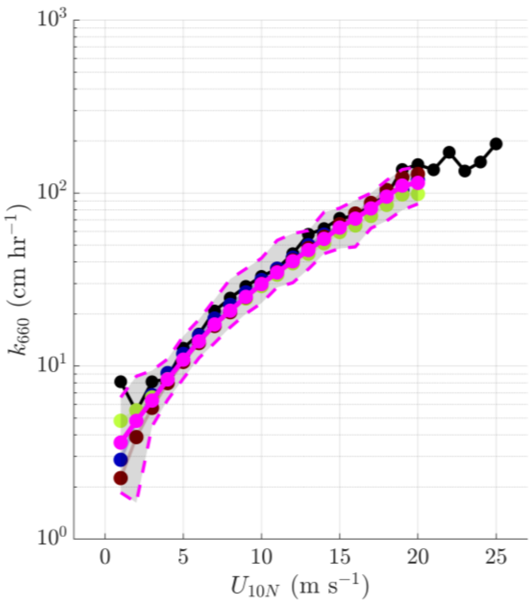

PDFs

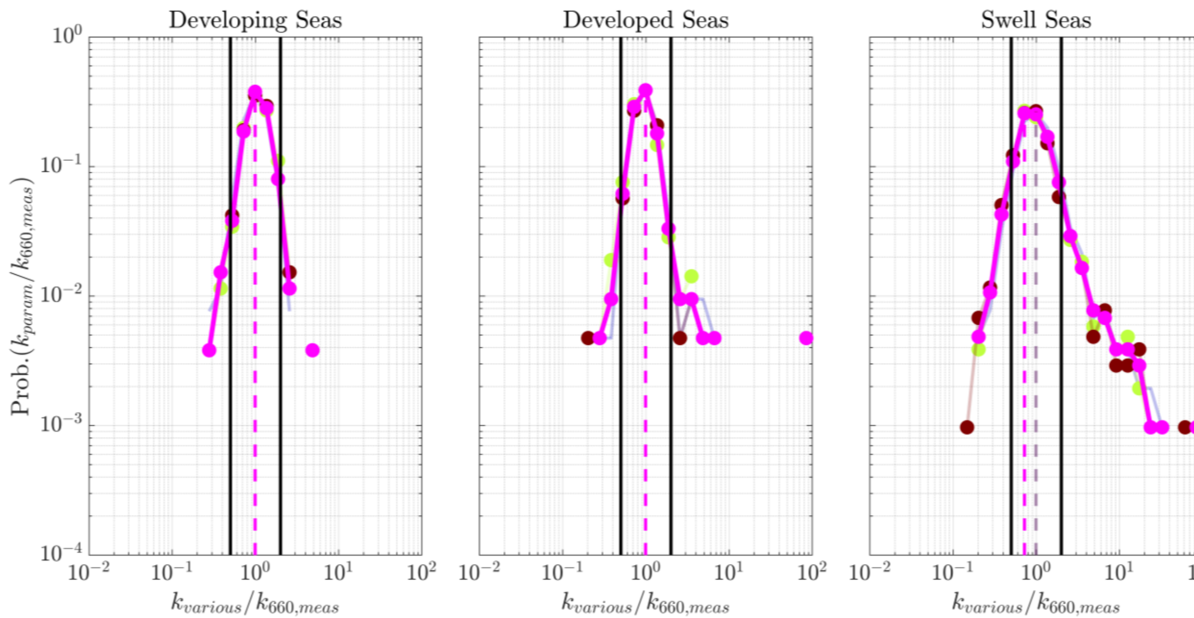

- φ =R^2/RMSE: SC23 outperforms F11 (by 9.7%) and DM18 (by 3.3%)
- Ensemble range larger at $U_{10N} \leq 4$ ms^{-1}, swell PDF shows low-wind over-estimation
- Additional spread emerges at $U_{10N} > 12$ ms^{-1} … swell underestimation by F11
- All parameterisations perform well where wave spectrum peak is wind-sea

Results: Sensitivity to Diffusive Gas Flux Parameterisation

k_{660} (U_{10N})

PDFs

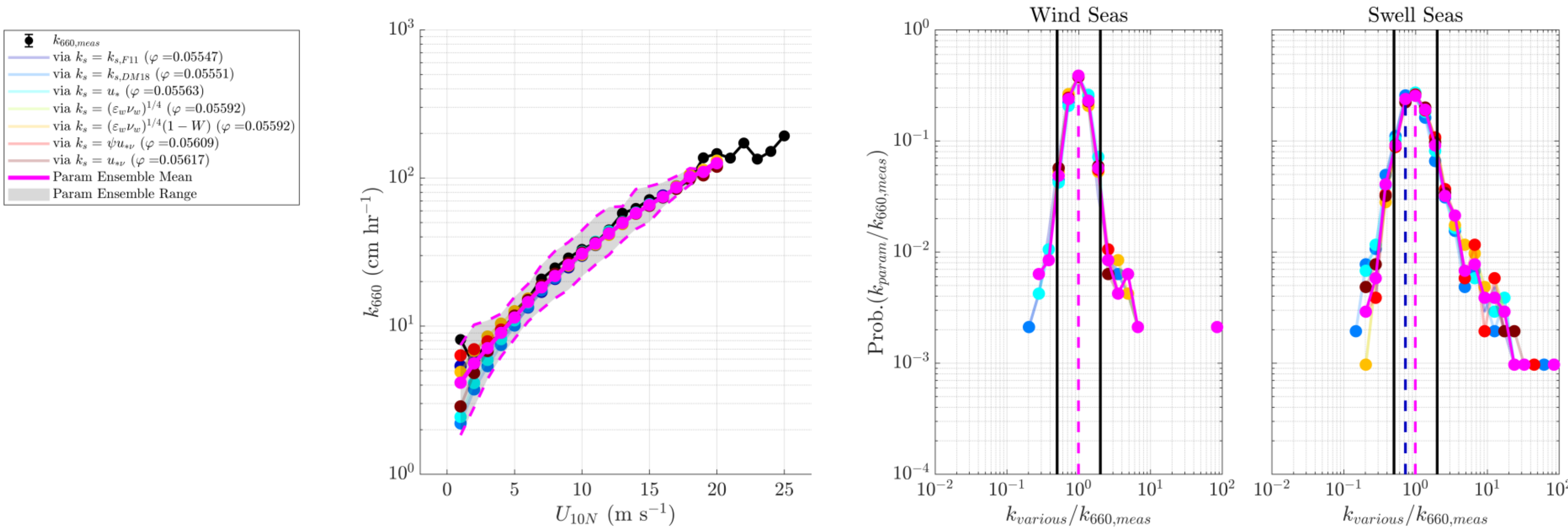

- Only 1.3% difference between worst-performing, best-performing via φ
- Greatest improvement: using $(\varepsilon_w \nu_w)^{1/4}$ vs. u_*, but dependent on which k_b you use
- Largest spread in ensemble at very low winds
- Ensemble convergence around U_{10N} = 12 ms^{-1}

Results: Sensitivity to Entrainment Velocity Choice

Parameterised vs. Observed k_{660}

PDFs

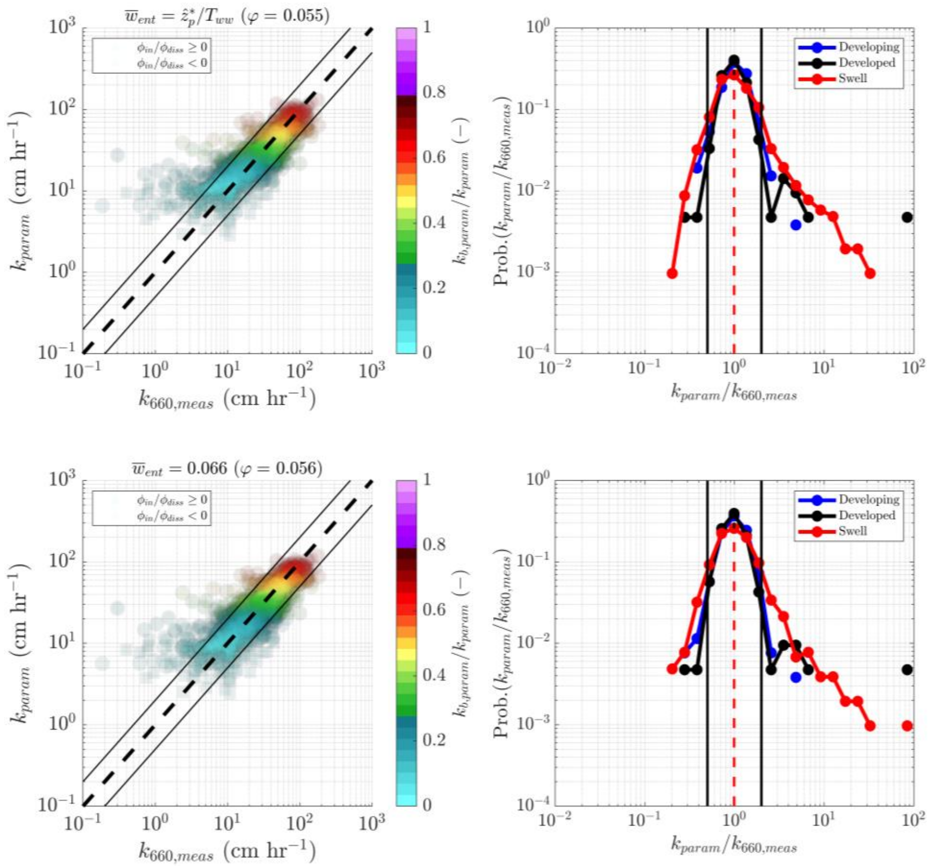

- Entrainment velocity either way almost visually identical and according to φ
- Using constant value reduces low-wind swell over-estimation somewhat
- Don't have to worry about the variability of z_p or T_{ww} by using constant

Results: Sensitivity to Growth-Phase Whitecap Fraction Parameterisation

k_{660} (U_{10N})

PDFs

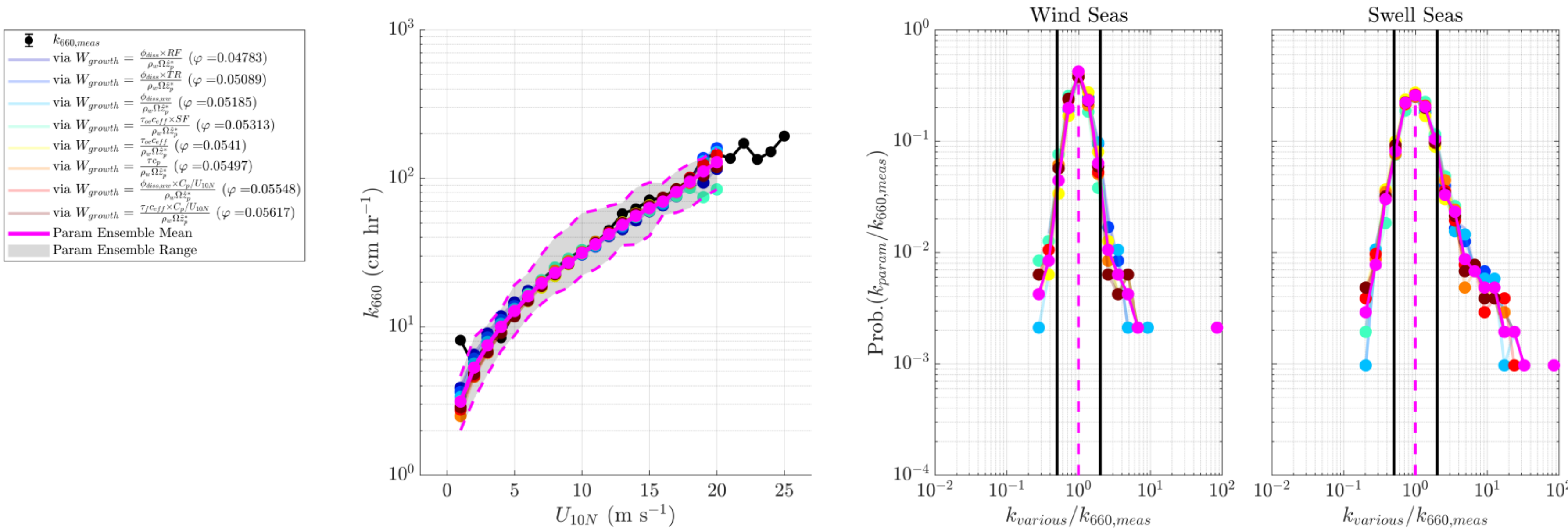

- Choice of W_{growth}: 17.4% difference between worst-performing, best-performing via φ
- Over-estimation of k at low winds using full φ_{diss} or omitting wave-age scaling in W_{growth}
- All similar for U_{10N} = 7-12 ms^{-1}; sample-size issue – very large spread at $U_{10N} \geq 18$ ms^{-1}
- Most impactful choice

Results: Sensitivity to Initial Bubble Injection Depth in Bubble Efficiency

k_{660} (U_{10N})

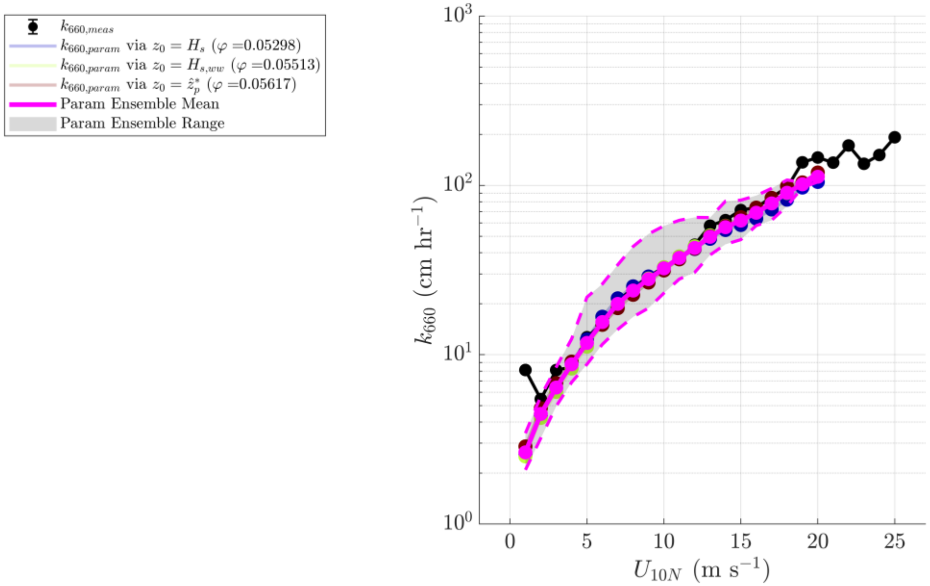

PDFs

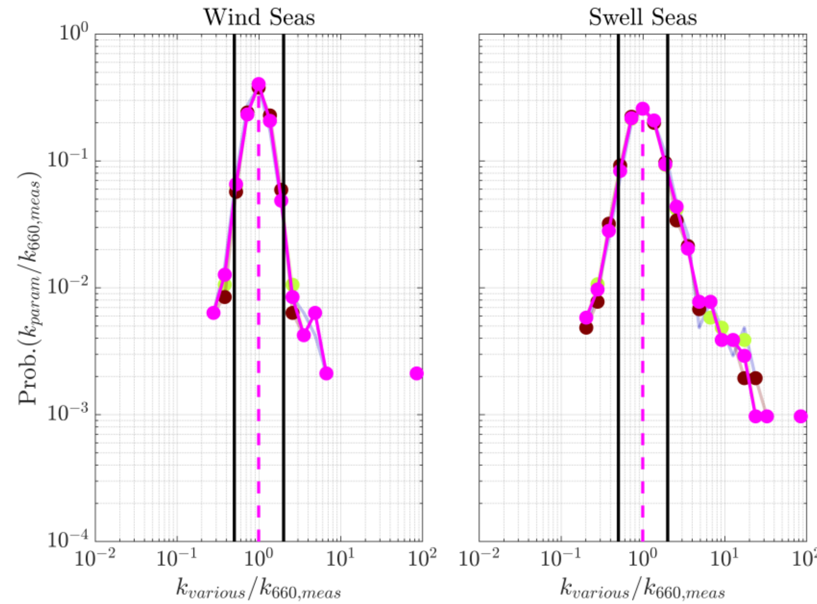

- z_0 in E(r) : 6% difference between worst-performing, best-performing via φ
- H_s *over-estimates* at low winds and *under-estimates* at high winds
- Bubble injection depth critically tied to wind-wave spectrum, higher-frequency waves
- Here, the choice is easy

Results: Sensitivity to Bubble Rise Velocity Parameterisation

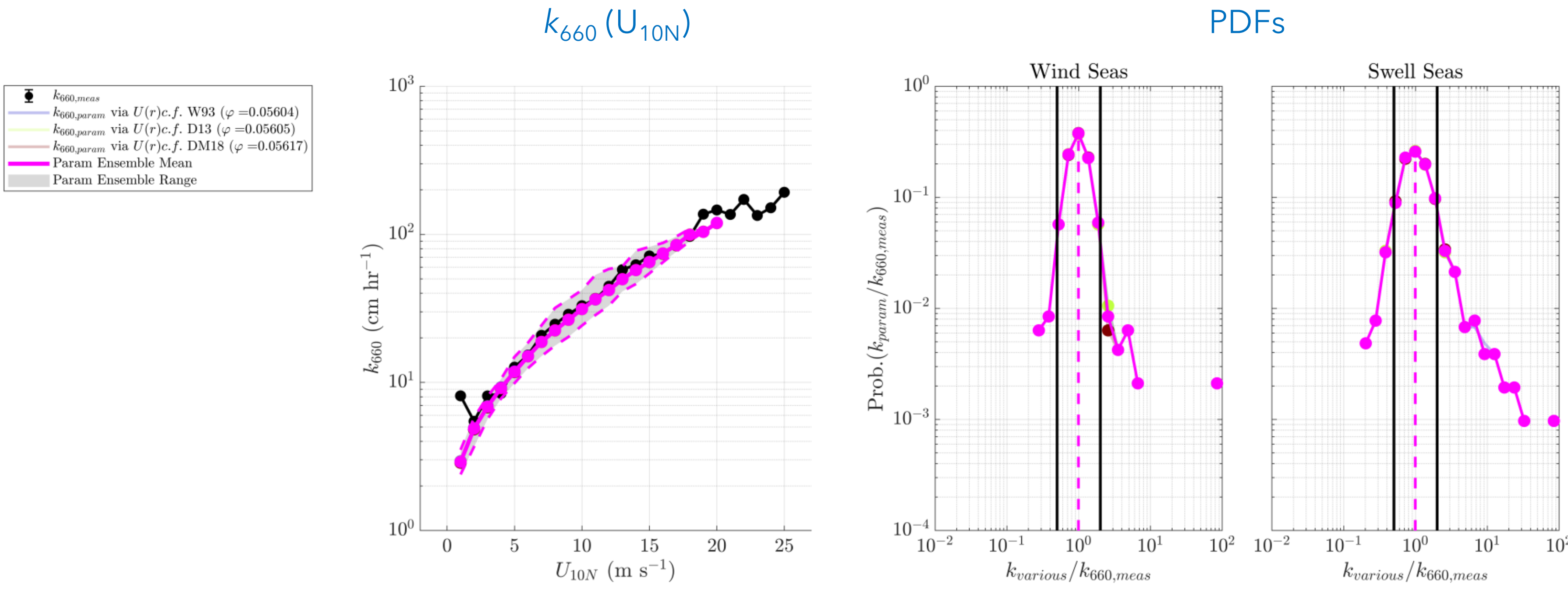

- Only 0.2% difference between worst-performing, best-performing via φ
- Bubble of constant radius, terminal velocity, quiescent liquid, clean or dirty (W93)
- Bubble of constant radius, terminal velocity, turbulent liquid, dirty (D13, DM18)
- Least numerically impactful choice, but considering surfactants physically important

Results: Total *k* Performance Matrix

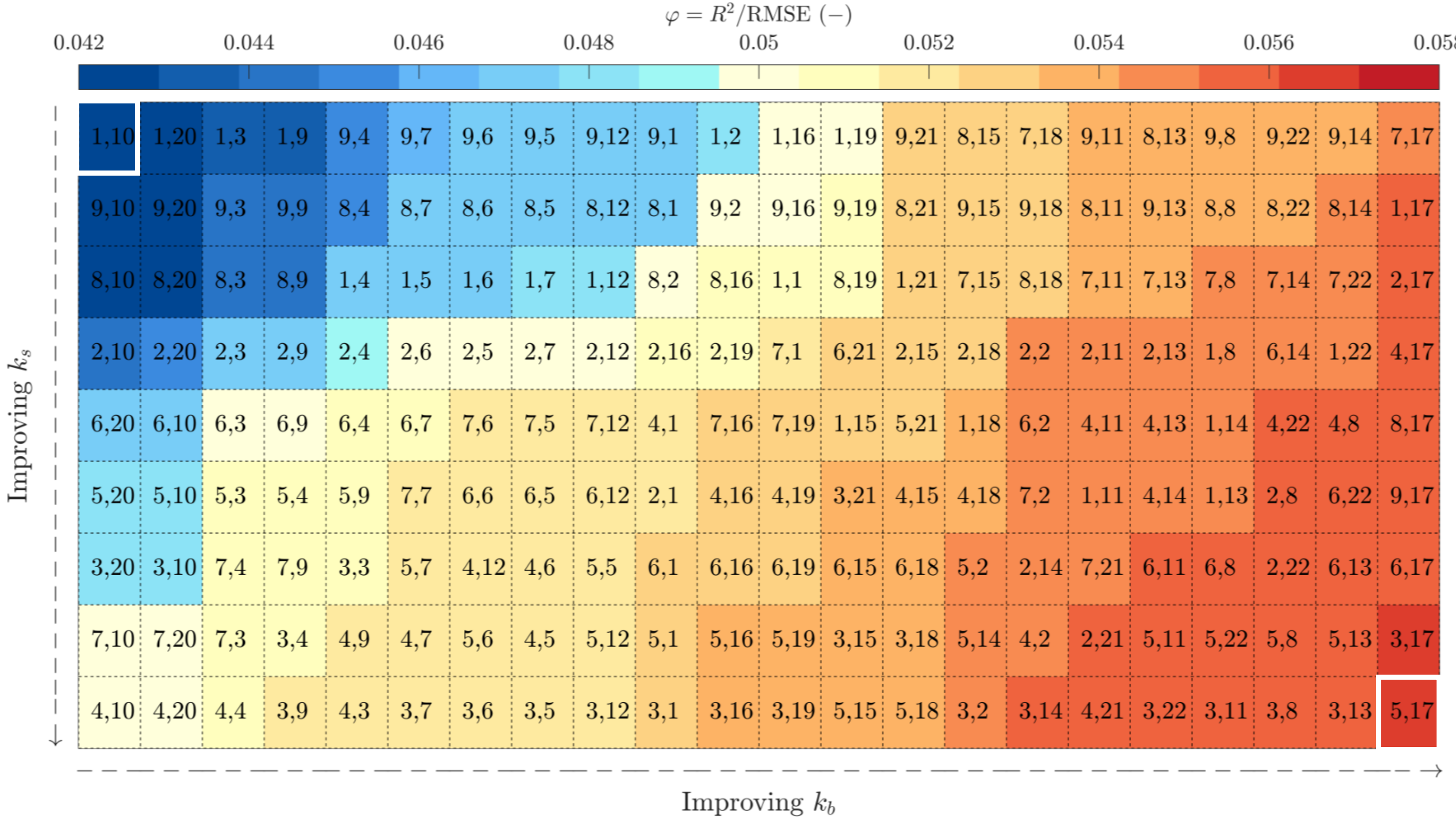

- Worst-performing overall: $k = 37.5 A\psi \cancel{u_{*\nu}} + c_2 \cancel{\frac{1}{\alpha}} \cancel{a_{eff}} [\overline{w}_{ent} \cancel{=} 0.066][W_{growth} = \frac{\phi_{diss} \times (\frac{H_{s,ww}}{H_{s,tot}})^2}{\cancel{\rho_w \Omega \hat{z}_p^*}}]\cancel{\xi}$
- Best-performing overall: $k = c_1 \cancel{u_{*\nu}} + c_2 \cancel{\frac{1}{\alpha}} \cancel{a_{eff}} [\overline{w}_{ent} \cancel{=} 0.066][W_{growth} = \frac{\tau_f c_{eff} \times (c_p U_{10N}^{-1})}{\cancel{\rho_w \Omega \hat{z}_p}}]\cancel{\xi}$

Conclusions

1. Diffusive gas transfer velocity inadequate by itself to parameterise *k*

2. Constant effective void fraction & entrainment velocity are reasonable to implement in bubble-mediated gas transfer velocity parameterisations

3. W_{growth} is the most important physical quantity to get correct

4. Bubble rise velocity least impactful choice to parameterisation performance

5. Optimised comparison of 198 parameterisations shows partition of stress in hybrid *k* parameterisations performs very well

Additional Links

Presentations

1

Investigating gas exchange processes using noble gases in very high winds: observations of bubbles and turbulence beneath breaking waves

2

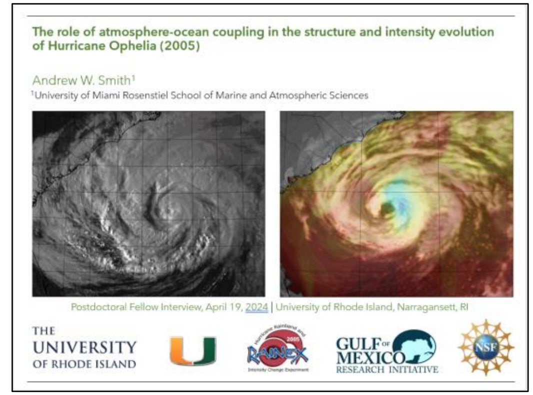

The role of atmosphere-ocean coupling in the structure and intensity evolution of Hurricane Ophelia (2005)

Associated Publications and Manuscripts

Smith, A. W., Haus, B. K., & Stanley, R. H. R. (2022). Bubble-turbulence dynamics and dissipation beneath laboratory breaking waves. *Journal of Physical Oceanography*, *1*, 2159–2181. https://doi.org/10.1175/JPO-D-21-0209.1

Stanley, R. H. R., Kinjo, L., Smith, A. W., Aldrett, D., Alt, H., Kopp, E., Krevanko, C., Cahill, K., & Haus, B. K. (2022). Gas fluxes and steady state saturation anomalies at very high wind speeds. *Journal of Geophysical Research: Oceans*, 1–19. https://doi.org/10.1029/2021jc018387

Smith, A. W. (2016). The role of air-sea interaction in structure and intensity change in Hurricane Ophelia (2005): Coupled modeling and RAINEX observations. https://scholarship.miami.edu/esploro/outputs/graduate/The-Role-of-Air-Sea-Interaction-in/991031447708902976?institution=01UOML_INST